PHYSICAL REVIEW A VOLUME 46, NUMBER 6 15 SEPTEMBER 1992

Experimental study of the signal-to-noise ratio of stochastic resonance systems

Gong De-chun
Department of Physics, Beijing Normal University, Beijing 100875, People's Republic of China

Hu Gang
Department of Physics, Beijing Normal University, Beijing 100875, People's Republic of China and Institute of Theoretical Physics, Academia Sinica, P.O. Box 2735, Beijing, People's Republic of China

Wen Xiao-dong, Yang Chun-yan, Qin Guang-rong, Li Rong, and Ding Da-fu
Department of Physics, Beijing Normal University, Beijing 100875, People's Republic of China
(Received 25 November 1991)

Electric analog circuits are used to simulate stochastic resonance (SR) systems. It is found that the signal-to-noise ratio (SNR) obtained by the SR device can exceed the upper limit of the SNR obtained by the optimal linear filter. By applying two SR devices successively, the SNR obtained by the SR devices may be about eight times larger than that of the optimal linear filter.

PACS number(s): 05.40.+j, 05.20.−y

I. INTRODUCTION

The phenomenon of stochastic resonance (SR) has attracted much attention in the study of fluctuating systems in the last decade. It has been found that under proper nonlinear conditions of the system, an increase in disorder of the input may result in an increase in order of the output [1–9]. Specifically, the output signal can be greatly enhanced (while the output noise can be considerably lessened) by suitably increasing the input noise. This active role played by noise seems to be striking and conceptionally meaningful. It is particularly interesting to seek possible applications of this peculiar phenomenon for practical purposes.

In many practical cases, we are not very interested in the amplitude of the signal itself since there are so many well-known approaches for amplifying a signal. The signal-to-noise ratio (SNR) often plays a more important role since this quantity represents the quality of a signal. Therefore, the interest in the SR problem has shifted to the SNR in current works [5–8]. To get a signal with SNR as high as possible is one of the central tasks in information theory. There had been a great variety of methods (mainly, linear treatments, for instance, linear filtering) dealing with the problem of increasing the SNR of a signal before the term SR was adopted. In the study of SR we find that the SR devices may also be used to accomplish this task. Hence, it is interesting to ask if the SR devices can work better than all the known methods.

Given an input

$$I(t)=U(t)+Q(t) , \tag{1.1}$$

where $Q(t)$ is a white noise

$$\begin{aligned} &\langle Q(t)\rangle=0 ,\\ &\langle Q(t)Q(t')=2D\delta(t-t') , \end{aligned} \tag{1.2}$$

a well-known theory predicts that the largest SNR obtained by the optimal linear filter reads

$$R_{LM}=P_S/P_n , \tag{1.3}$$

where P_S is the total signal power [10]

$$P_S=\frac{1}{2\pi}\int P_\omega d\omega , \tag{1.4a}$$

$$P_\omega=\int_{-\infty}^{\infty}\langle U(t)U(t+\tau)\rangle e^{i\omega\tau}d\tau , \tag{1.4b}$$

and P_n is the noise power of per unit spectrum

$$P_n=D/\pi . \tag{1.5}$$

In (1.4) P_ω is independent of t if we deal with a steady process. In this paper we consider a sinusoidal signal

$$U(t)=U\cos\Omega t . \tag{1.6}$$

Then Eqs. (1.4) can be specified as

$$P_\omega=\frac{\pi}{2}U^2[\delta(\omega+\Omega)+\delta(\omega-\Omega)] , \tag{1.7a}$$

$$P_S=\frac{1}{2\pi}\int_0^\infty P_\omega d\omega=\frac{U^2}{4} . \tag{1.7b}$$

which leads to

$$R_{LM}=\frac{\pi}{4}\frac{U^2}{D} . \tag{1.8}$$

Equation (1.8) serves as the absolute upper limit for linear devices. Any new devices which can exceed this limit must be of great interest in the problem of signal transference and reception. One may ask if the SR devices belong to the devices of this kind.

Let us consider a nonlinear system which has been extensively investigated in the study of SR so far,

$$\begin{aligned} &\dot{X}=ax-bx^3+I(t), \quad a,b>0\\ &I(t)=U\cos(\Omega t)+Q(t), \quad U>0 . \end{aligned} \tag{1.9}$$

The central problem to be answered in this presentation is whether the ratio

$$G = R_{\rm SR}/R_{LM} \tag{1.10}$$

can be larger than unity ($R_{\rm SR}$ represents the SNR of the output of the SR devices). If we get $G>1$, a more effective way of producing higher SNR is realized, and useful applications of the SR effect may be expected.

Gammaitoni *et al.* first used an electric circuit to simulate a periodically forced bistable stochastic system in the SR study [11–13]. This analog simulation has two advantages. On one hand, it is an experimental study. The result is more useful for application. On the other hand, it directly simulates a well-defined differential equation, and then allows a close comparison with theoretical analysis. Recently, Zhou and Moss [14], Gong *et al.* [15], and Hu *et al.* [16] also used an analog circuit to simulate Eq. (1.9).

The main purpose of the present paper is to experimentally (by using an electric circuit) investigate whether the quantity G can be larger than unity, and how G can be modified by changing the control parameters. In Sec. II we describe the experimental set and the method measuring the quantity G. In Sec. III we present experimental data of G. It will be shown that G can be considerably larger than unity. The influences of various control parameters on G are experimentally investigated. In Sec. IV we use two SR devices successively to treat the input signal and noise. It is found that both SR sets can effectively enhance the SNR.

II. EXPERIMENT DESIGN

Figure 1 shows the block of the analog circuit simulating Eq. (1.9), $U(t)$ and $H(t)$ are the signal and the noise sources, respectively. The output of the set is $X(t)$ which is the solution of Eq. (1.9). IC_1 is an operational integrator, IC_2 an inverter. D and E are two multipliers. In our simulation we adjust the experiment parameters to ensure $a=b=1$. In our experiment three quantities, U, f, and H, can be directly changed and measured. (1) The amplitude U and the frequency f [note, $U(t)=U\cos(ft+\theta)$] can be directly read from the signal generator. (2) The effective voltage of the noise H can be read from the noise generator. H can be changed in a wide regime. Of course, the noise generator can never produce true white noise since the total power of a white noise should be infinite. However, in our experiment the spectrum of the noise is uniformly distributed in the wide frequency interval $0-6f_0$, and then it can be approximately regarded as a white noise in our problem. In Fig. 2 we plot the spectrum of the noise at $H=3$ V.

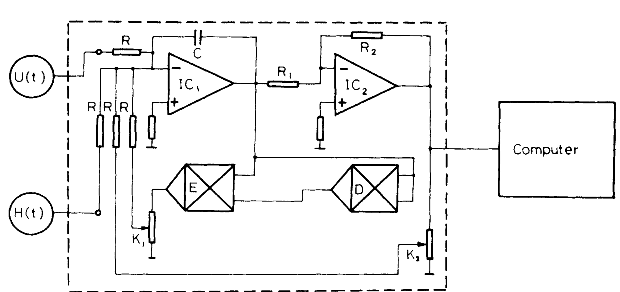

FIG. 1. The block diagram of experimental apparatus.

The experimentally measurable quantities are related to the parameters in Eq. (1.9) as follows:

$$f_0 \propto \Omega\ ,\qquad H \propto \sqrt{D}\ . \tag{2.1}$$

In this paper we are not interested in the proportion coefficients. Instead, we focus on the problem whether G can be larger than unity in certain parameter regions of U and H [i.e., certain parameter regions of U and D in Eq. (1.9)], and how large the maximal G can be. The frequency f is fixed to be $f_D=100$ Hz throughout the paper.

The output $X(t)$ is received by the computer through an analog-to-digital converter (ADC) where the spectrum of $X(t)$ is computed. For making fast Fourier transformation the computer collects 2000 data in $T=1$ sec. The experimental signal-to-noise ratio ($\bar{R}$) is defined as the ratio of the height of the spectrum of the output signal at frequency f_0 to the average amplitude of the background noise spectrum in the vicinity of f_0. $\bar{R}_{LM}$ is directly measured from the input $U(t)+H(t)$ while $\bar{R}_{\rm SR}$ is measured from the output of the SR device, $X(t)$.

We denote the experimentally measured signal-to-noise ratio quantities with an overbar. The experimental SNR is different from the SNR defined in Eqs. (1.3)–(1.5). First, the Fourier transformation of the experimental data is made in finite time interval T, and then the δ function in (1.7a) should be replaced by a spectrum peak of finite height proportional to T. Second, the Fourier transformation of the correlation function in (1.4b) is replaced by that of the $X(t)$ time sequence. (In this way we considerably save experimental and computing time.) However, by applying the Wiener-Khinchin theorem [17,18] and performing some elementary calculation we can relate the theoretical SNR(R) to the experimental SNR($\bar{R}$) as

$$R \propto \frac{1}{T}(\bar{R})^2\ . \tag{2.2}$$

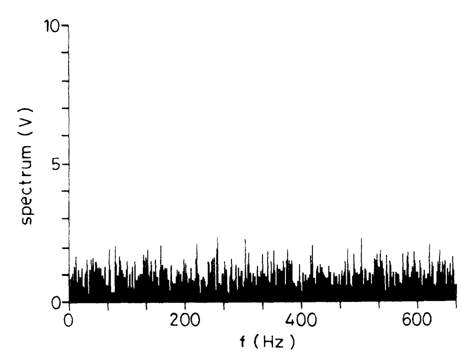

FIG. 2. The spectrum of noise output of the noise generator. $H=3$ V. The spectrum is practically uniform in the frequency interval $f<600\ \text{Hz}=6f_0$.

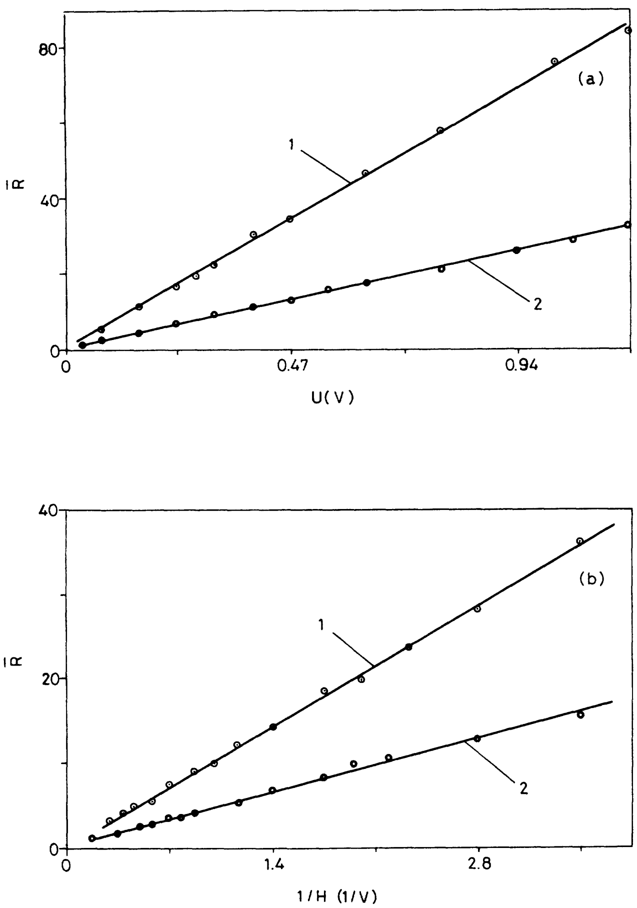

FIG. 3. (a) The SNR measured from the spectrum of the input $I(t)$ (represented by $\bar{R}_{LM}$), which is related to the SNR of the optimal linear filter by Eqs. (1.8) and (2.2), against U. $H=0.4$ V (curve 1) and $H=1.1$ V (curve 2). The linear dependence confirms the theoretical result. (b) $\bar{R}_{LM}$ (vs) $1/H$. $U=0.32$ V (curve 1) and 0.16 V (curve 2). The linear dependence is also consistent with Eqs. (1.8), (2.1), and (2.2).

[Note, R defined in (1.7) has the dimension of 1/sec while $\bar{R}$ is dimensionless.] Accordingly, the ratio of R_{SR} to R_{LM}, i.e., the quantity G, is related to $\bar{G}$ by

$$\bar{G}=\frac{\bar{R}_{\mathrm{SR}}}{\bar{R}_{LM}}=\left[\frac{R_{\mathrm{SR}}}{R_{LM}}\right]^{1/2}=(G)^{1/2} . \tag{2.3}$$

In the following, we focus on the experimental investigation of the behaviors of the quantities $\bar{R}$ and $\bar{G}$.

In Figs. 3(a) and 3(b) we plot $\bar{R}_{LM}$ against U and $1/H$ by fixing H and U, respectively. In both cases we find straight lines. These behaviors are consistent with the theoretical result (1.8) [together with (2.1) and (2.2)] and confirm the validity of our experiment design.

III. EXPERIMENTAL RESULTS BY USING ONE SR DEVICE

In Fig. 4(a) we fix $U=0.16$ V and plot $\bar{R}$ vs H. The crosses represent $\bar{R}_{\mathrm{SR}}$ while the circles represent $\bar{R}_{LM}$. Each plot is determined by the average of 20 measurements. Due to the statistical treatment the curves are quite smooth. A striking result demonstrated in the figure is that the crosses may be above the circles in a wide region of H. In Fig. 4(b) the amplitude of the input signal is raised to $U=0.32$ V. The general characters of the curves are similar to those in Fig. 4(a). In Fig. 5 we plot $\bar{G}$ vs H. Curves 1 and 2 correspond to $U=0.16$ and 0.32 V, respectively. A clear fact is that $\bar{G}$ can be considerably larger than unity.

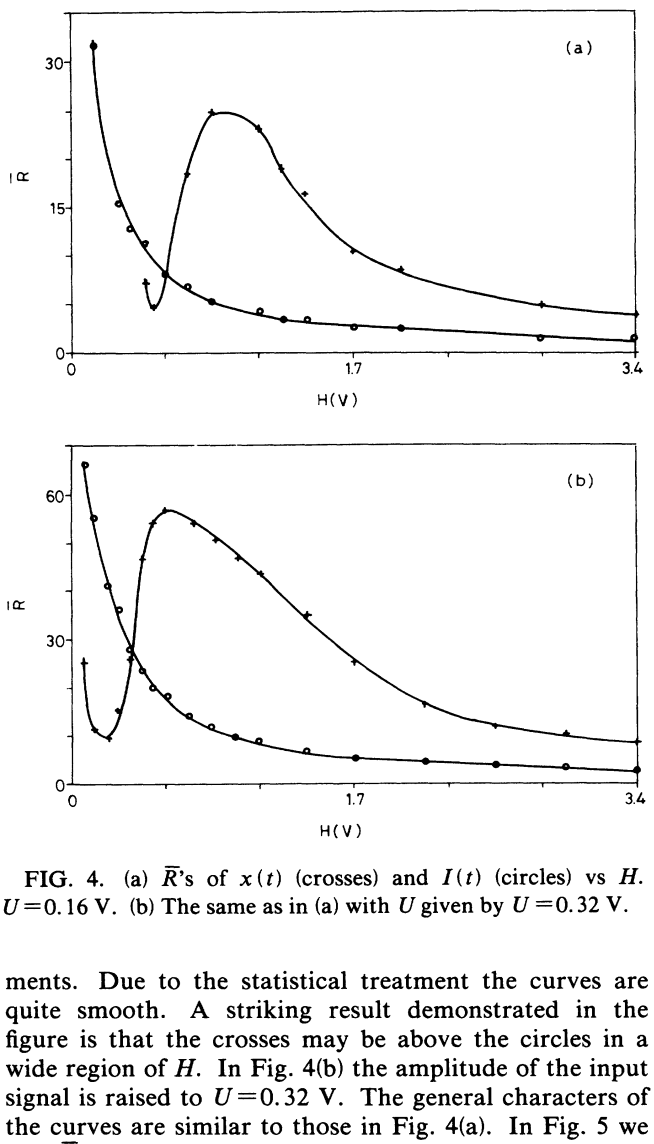

FIG. 4. (a) $\bar{R}$'s of $x(t)$ (crosses) and $I(t)$ (circles) vs H. $U=0.16$ V. (b) The same as in (a) with U given by $U=0.32$ V.

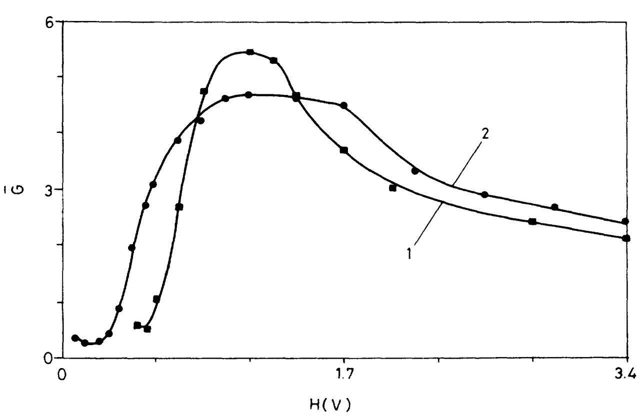

FIG. 5. $\bar{G}$'s given by Eqs. (2.3) and (1.10) against H. Curve 1 corresponds to $U=0.16$ V and curve 2 $U=0.32$ V. $\bar{G}>1$ in a wide region of large H.

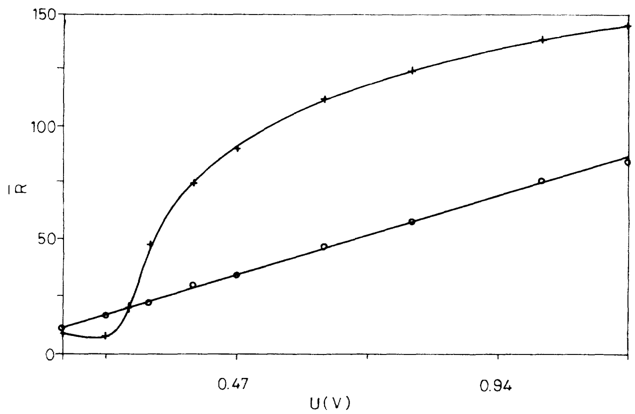

FIG. 6. $\bar{R}$'s of $x(t)$ and $I(t)$ vs U. $H=0.8$ V. In the cross curve, three scaling H regions can be clearly seen.

In Fig. 6 we plot $\bar{R}$ against U by fixing $H=0.8$ V. The crosses and circles have the same meanings as in Fig. 4. In Fig. 6 at relatively small H the cross curve demonstrates, obviously, three scaling regions. We find rare or random switchings in the first (small U) region, optimal switchings in the second (intermediate U) regions, and saturation in the third (large U) region. In the first region it is possible that increasing the input signal with the input noise fixed may result in decreasing experimental SNR of the output because of the random switchings. The second scaling region demonstrates obviously stochastic resonance where slightly increasing the input signal may lead to considerably increasing the output signal and the output experimental SNR. In Fig. 7 we plot $\bar{G}$ vs U. Again we find that $\bar{G}$ can be larger than unity in a wide U region. A manifest point is that $\bar{G}$ increases rapidly in the stochastic resonance region.

The reason why we can get $G>1$, or in other words, why we can get higher SNR by using the SR devices than the highest SNR obtained by linear devices can be understood from the mechanisms of both SR and linear devices. The way for a linear device to increase the SNR of a signal is to filter out certain parts of noise. The best

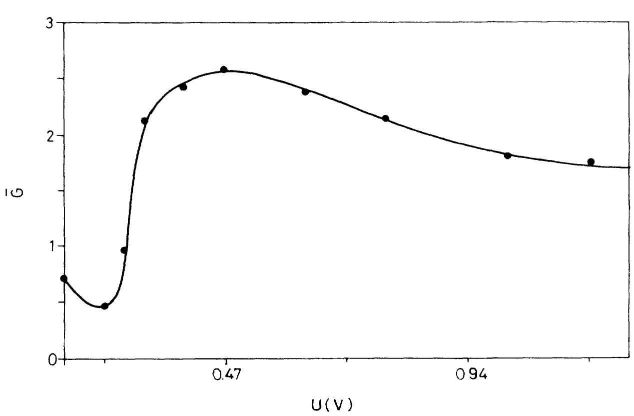

FIG. 7. $\bar{G}$ vs U. $H=0.8$ V.

filter [which gives the SNR in Eq. (1.8) if the signal and noise are given by (1.2) and (1.6)] can take away noise as much as possible. The mechanism of the SR device is completely different. The essential point is that this de-

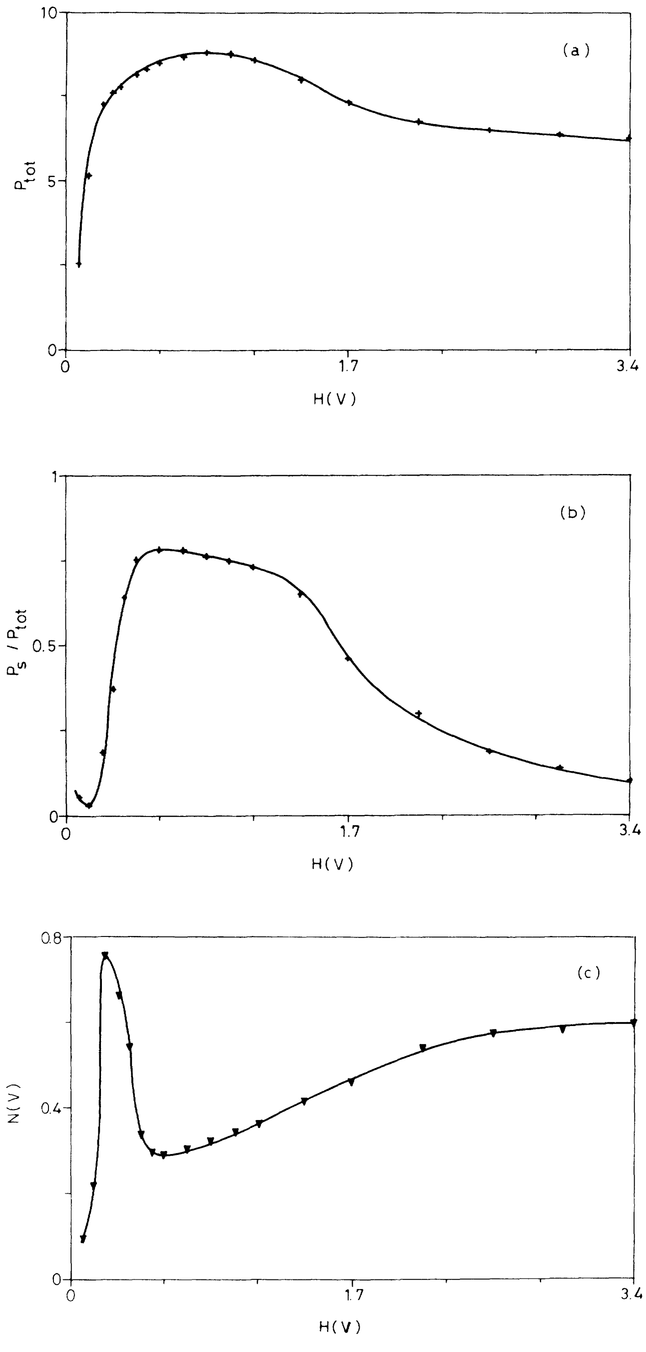

FIG. 8. (a) The total output power of the SR device vs H. $U=0.32$ V. The unit is not specified, and then only the relative height takes meaning. (b) The ratio of the signal power to the total power of the output of the SR device. There is a huge hump in the stochastic resonance region. In this region the energy transfer from noise to signal is obvious. (c) The average amplitude of the output noise spectrum of the SR device in the vicinity of the input frequency $f_0=100$ Hz. The output noise is considerably reduced in the stochastic resonance region.

vice allows an energy transfer from noise to signal under certain nonlinear conditions of the system. (For the theoretical description of this effect, see Ref. [6].) This energy transfer is particularly effective in enhancing the output signal and lessening the output noise. This fact has not been taken into account in previous analysis of the SNR of linear devices, to our knowledge.

From Fig. 8 the energy transfer in the SR device can be clearly seen. In Fig. 8(a) we plot the total power of the output P_{tot} against H with $U=0.32$ V. The P_{tot} increases rapidly as H increases from zero. Then the total power reaches a saturative value, and becomes insensitive to the change of the input noise strength. In Fig. 8(b) the portion of the signal power in P_{tot} is plotted versus H for the same U. A huge peak appears in the stochastic resonance region. Part of the signal power uses more than 75% of the total output power. At the same H the input signal power only uses a few percent of the input P_{tot}. The energy transfer in the SR region can be further confirmed in Fig. 8(c) where the average amplitude of the background spectra of the output noise in the vicinity of f_0 is plotted versus H. The deep valley of the curve in the SR region clearly shows the effective energy transfer from noise to the output signal.

Part of the above experimental observations can be analytically predicted. The detailed theoretical investigation considering the quantity G will appear in a forthcoming paper.

IV. EXPERIMENTAL RESULTS BY USING TWO SR DEVICES SUCCESSIVELY

In Sec. III we found that the SNR of a signal can be considerably enhanced by using a SR device. It is interesting to ask if one can further increase the SNR of the signal by successively using the SR sets one after the other. If the answer is positive a powerful device in improving the quality of the signal and in separating weak signals from strong noise can be hopefully designed. In this section we consider a set of two SR devices which is schematically drawn in Fig. 9. In Fig. 9, A and B are two analog circuits simulating the following equations:

$$
\begin{aligned}
x(t) &= a_1 x - b_1 x^3 + I(t) , \\
y(t) &= a_2 y - b_2 y^3 + k x(t) ,
\end{aligned}
\tag{4.1}
$$

where

$$
I(t) = U \cos(ft+\theta) + H(t) .
$$

The time series of $I(t)$, $x(t)$, and $y(t)$ are monitored and recorded. The computer can make Fourier transformations of these three time series. The systems are adjusted such that $a_1 = a_2 = b_1 = b_2 = 1$. The multiple coefficient k is varied so that for a given $x(t)$ the output $y(t)$ has the highest measured SNR.

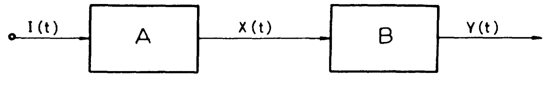

FIG. 9. The scheme of two-order stochastic resonance device. A and B are two blocks given in Fig. 1.

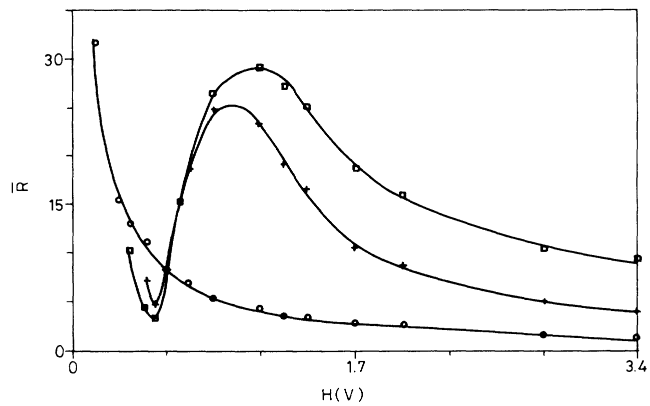

FIG. 10. The $\bar{R}$'s of $y(t)$ (squares), $x(t)$ (crosses), and $I(t)$ (circles) vs H. $U=0.5$ V.

In Fig. 10 we show the measured SNR's of $I(t)$ (circles), $x(t)$ (crosses), and $y(t)$ (squares) by varying H and fixing $U=0.16$ V. The highest measured SNR of the squares is slightly higher than that of the crosses. However, the peak of the squares is much flatter than that of the crosses. Therefore, the measured SNR of the output of the second SR device is considerably larger than that of the first SR device for relatively large H, which results in considerably enhancing the quantity $\bar{G}$. In Fig. 11 we plot $\bar{G}$ vs H for the same U. Curves 1 and 2 represent the $\bar{G}$'s of $x(t)$ and $y(t)$, respectively. It is clear that the second SR device can further increase $\bar{G}$. The quantity $\bar{G}$ of $Y(t)$ can increase eightfold, i.e., the successive use of two SR devices may lead to a measured SNR eight times higher than that obtained by the optimal linear filter.

In order to show how the SR devices can effectively enhance the SNR we present Figs. 12 and 13. In Fig. 12 we fix $U=0.16$ V, $H=2$ V. Figures 12(a)–12(c) give the spectra of $I(t)$, $x(t)$, and $y(t)$, respectively. In Fig. 12(a) the input signal is entirely submerged by the noise spectrum; meanwhile, the peaks of the signals of $x(t)$ and

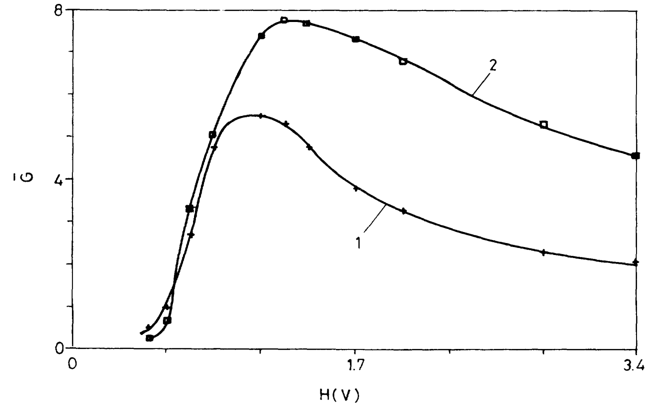

FIG. 11. $\bar{G}$'s plotted vs H. Curve 1 represents the ratio $\bar{R}_{\mathrm{SR}}[X(t)]/\bar{R}_{LM}$; curve 2 represents $\bar{R}_{\mathrm{SR}}[y(t)]/\bar{R}_{LM}$. The maximal $\bar{G}$ of curve 2 is 40% higher than that of curve 1.

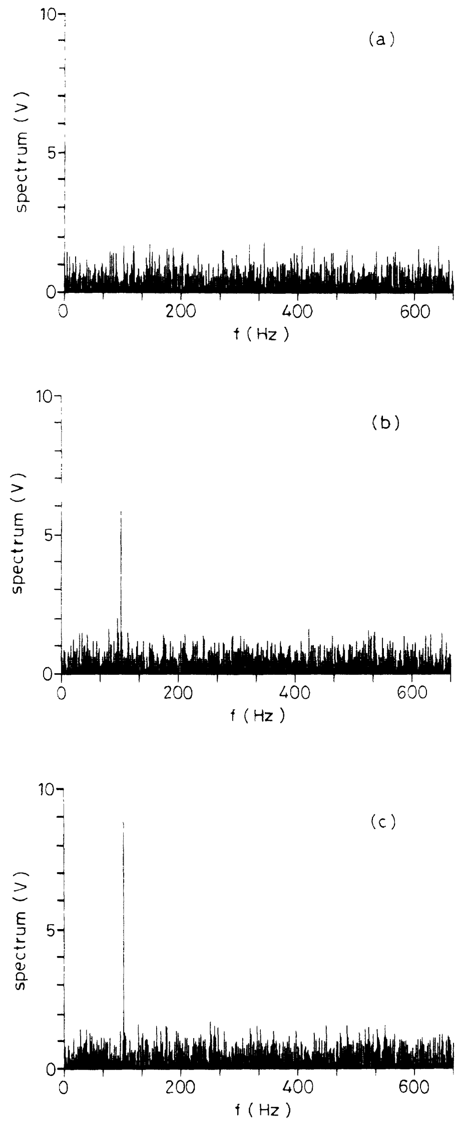

FIG. 12. The spectra of $I(t)$. (a), $X(t)$ (b), and $y(t)$ (c), respectively. $U=0.16$ V, $H=2$ V. In (a) the signal cannot be found. At the same parameters the signal spectra in (b) and (c) can be clearly seen.

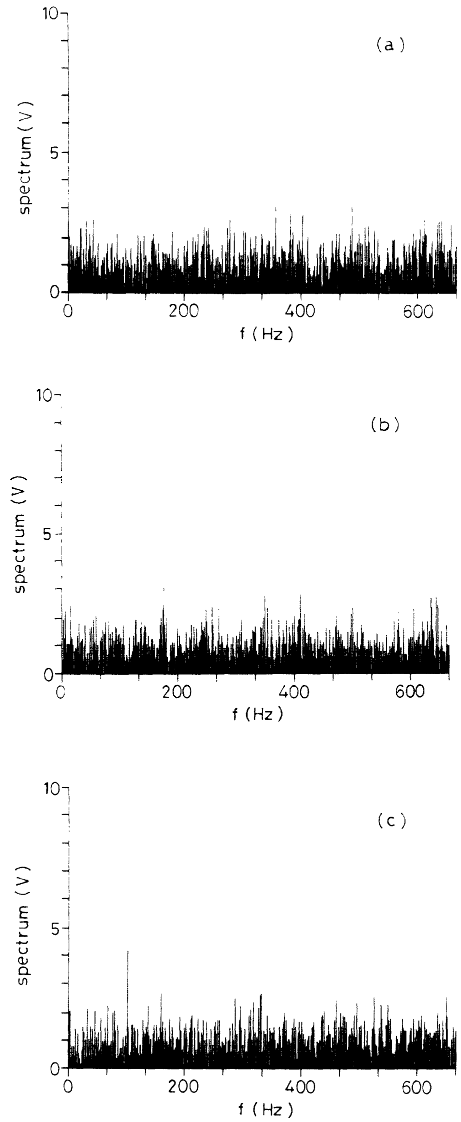

FIG. 13. The same as in Fig. 12 with H given by $H=5$ V. The signal spectra disappear in both (a) and (b). However, after the second SR device the signal spectrum clearly grows up out of the noise sea.

$y(t)$ are standing highly above the noise backgrounds in Figs. 12(b) and 12(c). In Fig. 13 we increase the input noise to $H=5$ V and keep the input signal unchanged. In both spectra of $I(t)$ and $x(t)$, one cannot see the trace of the signal. Nevertheless, the signal is manifest in the spectrum of the output $y(t)$. A clear impression is that the SR devices are really useful for improving the quality of the signal and for separating the weak signal from strong noise.

From Figs. 10 and 11 it is obvious that the second SR device is not as effective as the first one in enhancing the SNR. Actually, we find that the highest experimental SNR of the output of the first SR device can hardly be further increased by the second SR device. The reason is that the nature of the input of the second SR device (i.e., the output of the first SR device), $x(t)$, is considerably different from that of the input of the first device, $I(t)$. $Q(t)$ can be approximately regarded as a white noise, while the noise in $X(t)$ can never be regarded as white. The finite correlation time of the noise in $X(t)$ considerably reduces the efficiency of the second SR device. We believe that there must be a limit in enhancing the experimental SNR by successively using the SR devices. However, suitably using a combination of various nonlinear as well as linear devices and properly adjusting various parameters may produce even higher $\overline{G}$ by applying multiorder SR devices.

ACKNOWLEDGMENT

This work was supported by National Natural Science Foundation of China.

[1] R. Benzi, G. Parisi, A. Sutera, and A. Vulpiani, J. Phys. A **14**, 453 (1982).
[2] C. Nicolis and G. Nicolis, Tellus **33**, 225 (1981).
[3] S. Fauve and F. Heslot, Phys. Lett. **97A**, 5 (1983).
[4] P. Jung and P. Hanggi, Europhys. Lett. **8**, 505 (1989).
[5] B. McNamara, K. Wesenfeld, and R. Roy, Phys. Rev. Lett. **60**, 2626 (1988).
[6] B. McNamara and K. Wiesenfeld, Phys. Rev. A **39**, 4854 (1989).
[7] R. Fox, Phys. Rev. A **39**, 4148 (1989).
[8] G. Hu, G. Nicolis, and C. Nicolis, Phys. Rev. A **42**, 2030 (1990).
[9] P. Jong and P. Hänggi, Phys. Rev. A **44**, 8032 (1991).
[10] D. F. Ding, Acta Phys. Sin. **24**, 431 (1975).
[11] L. Gammaitoni, F. Marchesoni, E. Menichella-Saetta, and S. Santucci, Phys. Rev. Lett. **52**, 349 (1989).
[12] L. Gammaitoni, E. Menichekka-Saetta, S. Santucci, F. Marchesoni, and C. Presilla, Phys. Rev. A **40**, 2114 (1989).
[13] L. Gammaitoni, M. Martinelli, L. Pardi, and S. Santucci, Phys. Rev. Lett. **67**, 1799 (1991).
[14] T. Zhou and F. Moss, Phys. Rev. A **41**, 4255 (1990).
[15] D. C. Gong, G. R. Qin, G. Hu, and X. D. Weng, Phys. Lett. A **159**, 147 (1991).
[16] G. Hu, G. R. Qing, D. C. Gong, and X. D. Weng, Phys. Rev. A **44**, 6424 (1991).
[17] N. Wiener, Acta Math. **55**, 117 (1930).
[18] S. R. de Groot and P. Mazur, *Nonequilibrium Thermodynamics* (North-Holland, Amsterdam, 1969).